

Accepted Manuscript

Discovery of Novel Simplified Isoxazole Derivatives of Sampangine as potent Anti-cryptococcal Agents

Zhuang Li, Na Liu, Jie Tu, Changjin Ji, Guiyan Han, Yan Wang, Chunquan Sheng

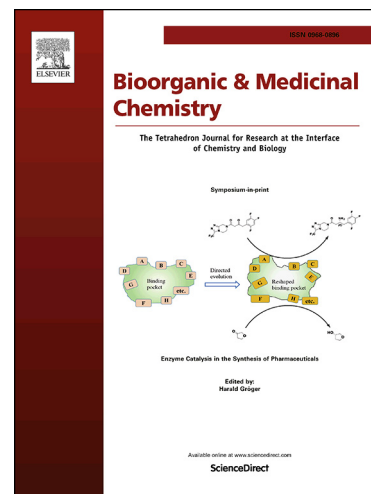
PII: S0968-0896(18)32120-5
DOI: <https://doi.org/10.1016/j.bmc.2019.01.029>
Reference: BMC 14721

To appear in: *Bioorganic & Medicinal Chemistry*

Received Date: 20 December 2018
Revised Date: 19 January 2019
Accepted Date: 23 January 2019

Please cite this article as: Li, Z., Liu, N., Tu, J., Ji, C., Han, G., Wang, Y., Sheng, C., Discovery of Novel Simplified Isoxazole Derivatives of Sampangine as potent Anti-cryptococcal Agents, *Bioorganic & Medicinal Chemistry* (2019), doi: <https://doi.org/10.1016/j.bmc.2019.01.029>

This is a PDF file of an unedited manuscript that has been accepted for publication. As a service to our customers we are providing this early version of the manuscript. The manuscript will undergo copyediting, typesetting, and review of the resulting proof before it is published in its final form. Please note that during the production process errors may be discovered which could affect the content, and all legal disclaimers that apply to the journal pertain.



**Discovery of Novel Simplified Isoxazole Derivatives of Sampangine as potent
Anti-cryptococcal Agents**

Zhuang Li^{1, †}, Na Liu^{2, †}, Jie Tu², Changjin Ji², Guiyan Han², Yan Wang^{2,*}, Chunquan Sheng^{1,2,*}

¹ *School of Pharmacy, Fujian University of Traditional Chinese Medicine, 1 Qiuyang Road, Fuzhou, Fujian 350122, P. R. China*

² *School of Pharmacy, Second Military Medical University, 325 Guohe Road, Shanghai 200433, People's Republic of China*

[#]These two authors contributed equally to this work.

* To whom correspondence should be addressed.

For C. Q. Sheng: Phone/Fax, 86-21-81871205, E-mail, shengcq@smmu.edu.cn;

For Y. Wang: Phone/Fax, 86-21-81871260, E-mail, wangyansmmu@126.com;

Abstract

Cryptococcus neoformans is the leading cause of cryptococcal meningitis, which is associated with high mortality due to lack of effective treatment. Herein a series of tricyclic isoxazole derivatives with excellent anti-cryptococcal activities were identified by structural simplification and scaffold hopping of antifungal natural product sampangine. Particularly, compound **8a** showed promising features as an anti-cryptococcal lead compound. It was highly active against *C. neoformans* ($\text{MIC}_{80} = 0.031 \mu\text{g/mL}$), which was more potent than fluconazole and voriconazole. Moreover, compound **8a** showed potent fungicidal activity and had potent inhibitory effects against important virulence factors (i.e. biofilm, melanin and urease) of *C. neoformans*. Preliminary antifungal mechanism investigation revealed that compound **8a** induced apoptosis of *C. neoformans* cells and arrested the cell cycle at the G1/S phase.

Keywords: structural simplification, anti-cryptococcal, fungicidal activity, virulence factors, antifungal mechanism.

1. Introduction

In the past few decades, the incidence of life-threatening invasive fungal infections (IFIs) has increased dramatically.^{1, 2} It was reported that serious fungal infections were mainly caused by species of *Candida*, *Cryptococcus*, *Aspergillus*, and *Pneumocystis*.³ Cryptococcal meningitis (CM) is an important mycosis worldwide caused by *Cryptococcus neoformans* (*C. neoformans*) and *Cryptococcus gattii* (*C. gattii*) with over 1 million cases and 600,000 deaths per year.⁴⁻⁶ Moreover, CM is a life-threatening disease in immunosuppressed patients and always associated with high mortality due to the lack of effective treatment.^{7, 8} Currently, clinically available therapy and maintenance regimens for CM mainly include amphotericin B (AMB), flucytosine and fluconazole (FLC).^{9, 10} However, each of these antifungal agents has significant adverse effects. For example, AMB is associated with infusional toxicity and renal impairment.¹¹ Bone marrow suppression can occur during 5-flucytosine therapy. FLC is fungistatic rather than fungicidal in the normal human dose range, which may cause hepatotoxicity.^{4, 9} The newly developed β -1,3-glucan synthase inhibitors (i.e. echinocandins) have poor effect against *Cryptococcus* species.^{12, 13} Thus, there is an urgent imperative to discover new molecules to treat cryptococcal infections.^{14, 15}

Natural products are potential sources of new antifungal drugs.¹⁶ For example, polyenes and echinocandins, two important types of antifungal agents, originated from natural products. However, complex chemical structures of natural products often lead to difficulties in chemical synthesis and unfavorable physicochemical properties.¹⁷ Thus, designing simplified derivatives of natural products with similar or even better antifungal activity represents an effective but challenging strategy. Previously, our group reported a successful example of structural simplification of natural product sampangine.¹⁸⁻²⁰ The simplified tricyclic pyridine derivatives (e.g. compound **3**) showed excellent

antifungal activities against *Candida albicans* (*C. albicans*). However, structure-activity relationship (SAR) for the anti-cryptococcal activity remains to be further investigated. Herein scaffold hopping of tricyclic pyridines was performed by replacing pyridine with isoxazole. Interestingly, the novel tricyclic isoxazole derivatives were highly potent and selective against *C. neoformans*. Particularly, compound **8a** (*C. neoformans*, MIC₈₀ = 0.031 µg/mL, **Fig. 1**) showed potent anti-cryptococcal activity, representing a promising lead compound for the development of novel CM therapeutic agents. SAR and preliminary mechanism of action of compound **8a** was also clarified.

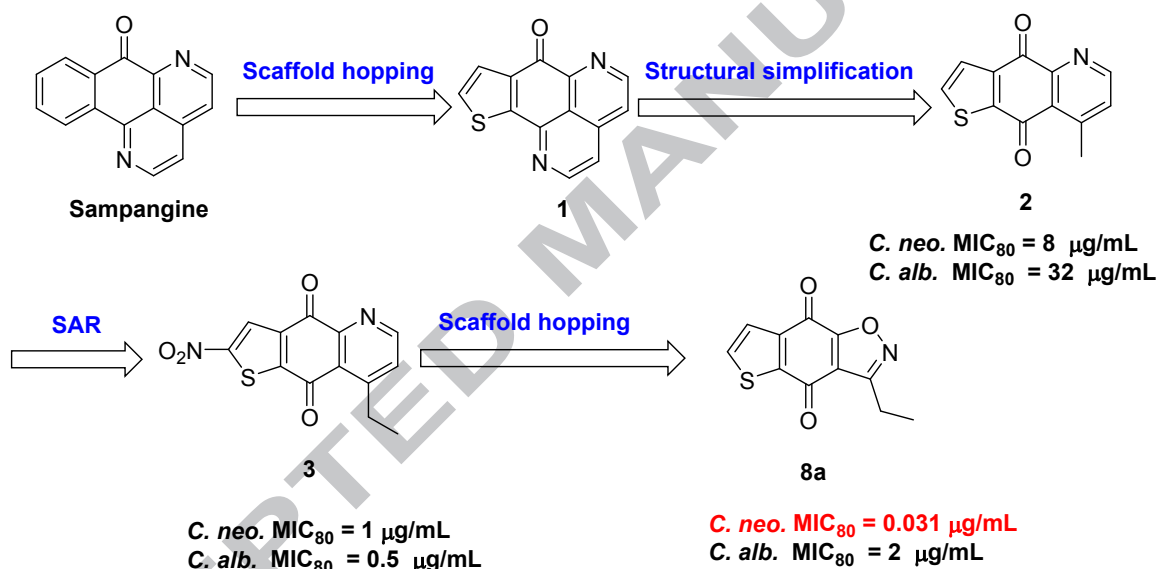
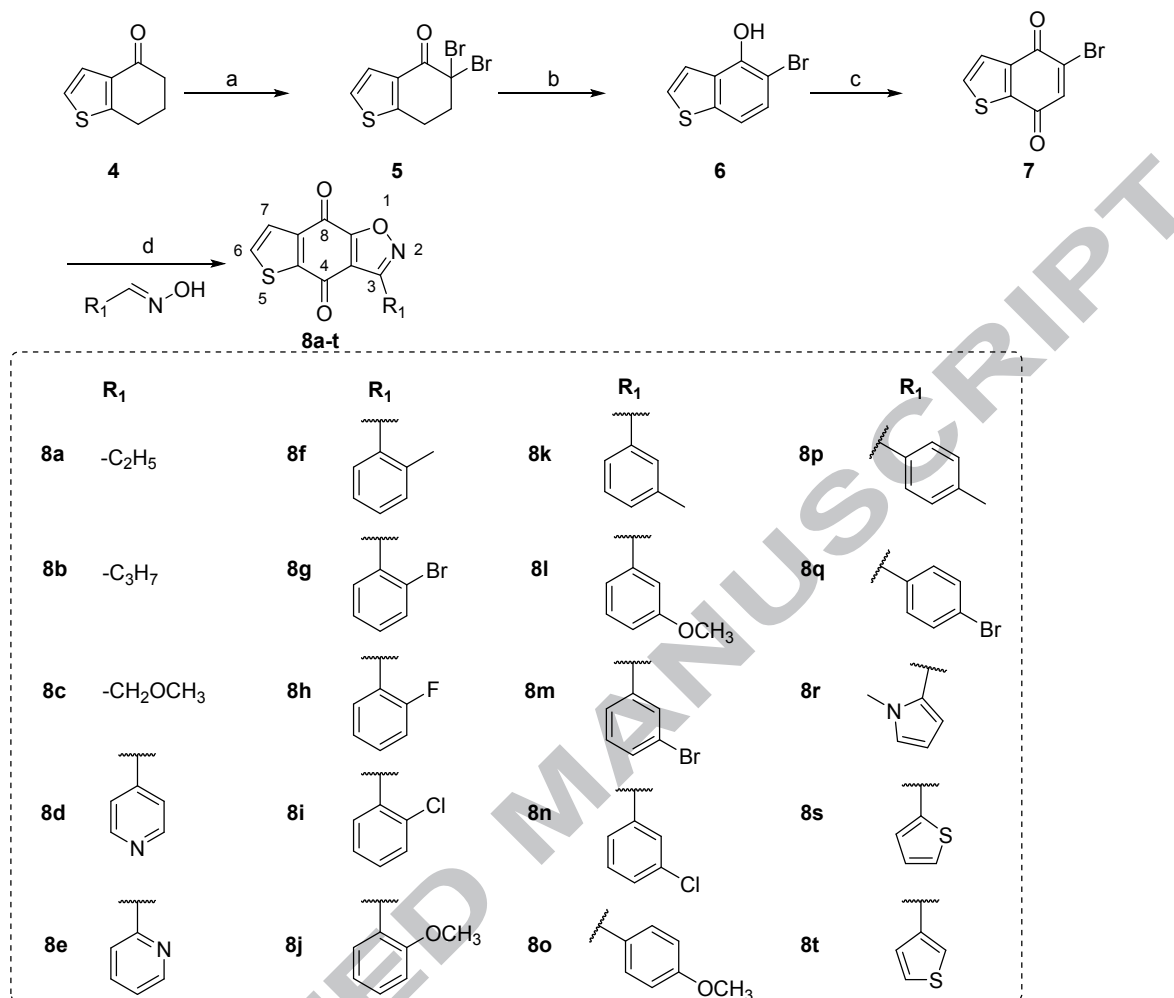


Fig. 1 Structural simplification processes of sampangine.

2. Chemistry

The chemical synthesis of tricyclic isoxazole derivatives is depicted in **Schemes 1**. Intermediates (**7**) were synthesized from substituted thienocyclohexanone (**4**) via three steps according to our reported methods.²⁰ Then, target compounds **8a-t** were prepared by reacting intermediates **7** with substituted aldoximes by a [1+2] cycloaddition reaction in the presence of NaClO (**Scheme 1**).



Scheme 1. Reagents and conditions: (a) CuBr₂, EtOAc/CHCl₃, 80 °C, 12 h, 92.1%; (b) Li₂CO₃, DMF, 100 °C, 6 h, 90.3%; (c) PhI(OAc)₂, HOAc/TFA, 0-25 °C, 0.5 h, 69.7%; (d) NaClO, Et₃N, DCM, 0-25 °C, 12 h, 21.7% ~ 82.4%.

3. Results and discussion

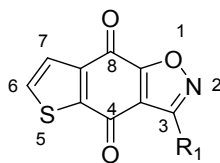
3.1. Scaffold hopping, *in vitro* antifungal activities and SAR

In vitro antifungal activities of the isoxazole derivatives were assayed against two fungal strains *C. albicans* SC5314 and *C. neoformans* H99 using triazole antifungal agents FLC and voriconazole (VRC) as the positive controls (**Table 1**). The minimum inhibitory concentration that achieved 80% inhibition (MIC₈₀) is used to express the *in vitro* antifungal efficacy. Initially, compound **8a** was designed by scaffold hopping of compound **3**, in which the pyridine group of the tricyclic scaffold

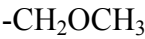
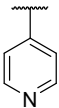
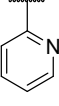
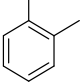
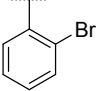
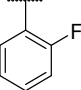
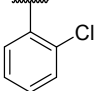
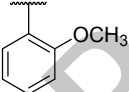
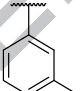
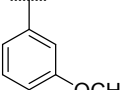
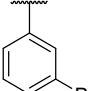
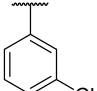
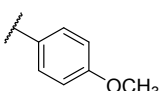
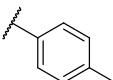
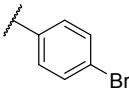
was replaced by isoxazole. Moreover, the aromatic nitro group was removed due to its potential risk to cause toxicity. Interestingly, compound **8a** was highly active against *C. neoformans* ($\text{MIC}_{80} = 0.031 \mu\text{g/mL}$), whereas its activity against *C. albicans* ($\text{MIC}_{80} = 2 \mu\text{g/mL}$) was slightly decreased as compared with compound **3**. The SAR was different from that observed in the tricyclic pyridine derivatives, in which the nitro group was found to be essential for the antifungal activity.²⁰ Inspired by the results, a series of tricyclic isoxazole derivatives were synthesized and assayed. Most compounds showed good to excellent antifungal activity against *C. neoformans*, whose activity was significantly better than that against *C. albicans* (Table 1).

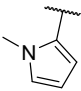
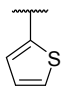
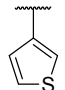
Various substitutions on the isoxazole ring (**8a-t**) were explored. Alkyl substitutions were more favorable for the anti-cryptococcal activity than the heterocycle and substituted phenyl derivatives, in which the ethyl substitution gave the best results. Among the substituted phenyl groups, ortho-substitution was better than meta- and para-substitutions. Meta-substituted derivatives **8l**, **8m** and **8n** were totally inactive. Among the target compounds, compound **8a** showed the best antifungal activity against *C. neoformans* H99 ($\text{MIC}_{80} = 0.031 \mu\text{g/mL}$), which was 64-fold more potent than FLC and 4-fold more potent than VRC (Table 1-2).

Table 1 *In vitro* antifungal activity of targets compounds **8a-t** (MIC_{80} , $\mu\text{g/mL}$)^a



Compound	R_1	<i>C. neo.</i>	<i>C. alb.</i>
		(H99)	(SC5314)
8a	$-\text{C}_2\text{H}_5$	0.031	2
8b	$-\text{C}_3\text{H}_7$	0.12	4

8c		0.25	8
8d		0.25	8
8e		0.25	8
8f		0.25	>64
8g		0.25	>64
8h		0.25	>64
8i		0.25	>64
8j		0.5	>64
8k		1	>64
8l		>64	>64
8m		>64	>64
8n		>64	>64
8o		1	>64
8p		1	>64
8q		>64	>64

8r		4	16
8s		2	>64
8t		1	>64
FLC	—	2	0.25
VRC	—	0.12	0.12

^a Abbreviations: *C. neo.*, *Cryptococcus neoformans*; *C. alb.*, *Candida albicans*.

3.2. Isoxazole derivatives showed excellent antifungal activities against *C. neoformans* var. *grubii* and *C. gattii*

According to the results of MIC₈₀ listed in **Table 1**, compounds **8a-d** were chosen to further evaluate the antifungal activity against *C. neoformans* var. *grubii* and *C. gattii*. These compounds had MIC₈₀ values in the range of 0.12–0.5 µg/mL, which were superior to FLC and comparable to VRC (**Table 2**). On the basis of the anti-cryptococcal activity, compound **8a** was chosen to further biological evaluations.

Table 2 *In vitro* antifungal activity of part of the target compounds (MIC₈₀, µg/mL)

Compound	<i>C. neo. var. Grubii</i>	<i>C. gattii.</i>
	(ATCC 34877)	(ATCC 14116)
8a	0.12	0.25
8b	0.12	0.25
8c	0.25	0.5

8d	0.5	1
FLC	8	8
VRC	0.12	0.12

3.3. Compounds **8a** and **8b** showed effective inhibitory effect on the biofilm formation of *C. neoformans*

Biofilm, an important virulence factor of fungi, is often related with drug resistance and repeated fungal infections in clinic.²¹ Thus, effects of compounds **8a** and **8b** on the formation of cryptococcal biofilms were evaluated. Considering that fluconazole had poor effects in inhibiting biofilm formation assay, AmB, a potent biofilm inhibitor, was chosen as the positive control. The results showed that they could significantly inhibit the biofilms formation, which was better than AMB. In particular, compound **8a** had an inhibition rate of more than 80% at the concentration of 0.062 $\mu\text{g/mL}$ (Fig. 2).

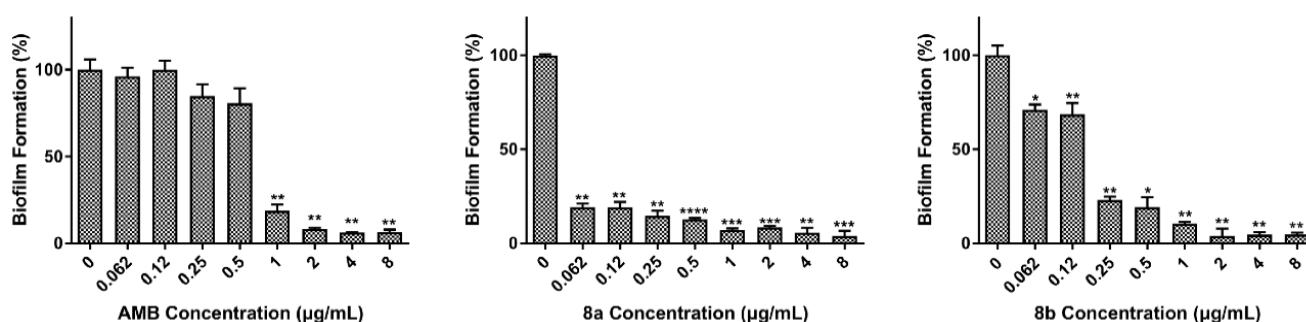


Fig. 2. Effects of different concentrations of compounds **8a**, **8b** and AMB on biofilm formation. *C. neoformans* H99 cells were treated with compound **8a**, **8b** and AMB (0.062-8 $\mu\text{g/mL}$). The results of biofilms formation are represented the means \pm standard deviations for three independent experiments. Statistical differences among groups were determined by ANOVA. The comparison

between the two components was completed by *t*-test. * $p < 0.05$; ** $p < 0.01$; *** $P < 0.001$; **** $P < 0.0001$ compared to the control group.

3.4. Compound **8a** inhibited the production of melanin and urease of *C. neoformans*

Melanin and urease are important virulence factors of *C. neoformans*. Melanin plays an indispensable role in protecting microorganisms from multiple toxic damages. It showed antioxidant function to defense environmental impurities and oxidative stresses.^{22, 23} Urease can increase the viability of *C. neoformans* in phagolysosomes.²⁴ Different induction mediums were used to induce melanin and urease production, respectively. As shown in **Fig. 3A**, if the cells produced melanin, the colonies would appear black on the melanin induction medium. Conversely, the colonies appear white. The results revealed that compound **8a** inhibited the production of melanin at the concentration of 16 $\mu\text{g/mL}$. As shown in **Fig. 3B**, if the cells produced urease, the medium would appear red. The results also showed that compound **8a** was able to inhibit the production of urease at the concentration of 64 $\mu\text{g/mL}$. (**Fig. 3B**).

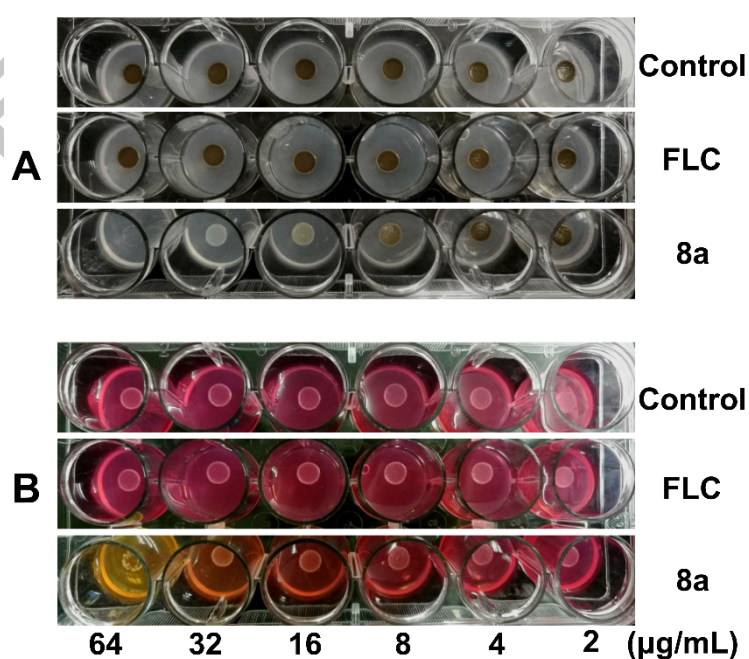


Fig. 3. Effects of compound **8a** on melanin and urease production by *C. neoformans* H99 cells. (A) *C. neoformans* H99 cells grown on L-DOPA medium were treated with different concentrations of compound **8a** to determine melanin production. (B) Strains grown on urea medium were used to determine the production of urease.

3.5. Compound **8a** exhibited fungicidal activity against *C. neoformans*

Time-growth curves were assayed to further evaluate the fungistatic activity of compound **8a**. As shown in **Fig. 4A**, different concentrations of compound **8a** (0.062-1 $\mu\text{g/mL}$) were used in time-growth curves assay. The results showed that the fungistatic activity of compound **8a** at 0.25 $\mu\text{g/mL}$ was superior to FLC at 16 $\mu\text{g/mL}$. Compound **8a** effectively inhibit *C. neoformans* H99 cells growth in a concentration-dependent manner, and completely inhibit H99 cells growth at 1 $\mu\text{g/mL}$. Meanwhile, time-kill curves assay was used to test whether compound **8a** had fungicidal activity. The FLC group (4 and 16 $\mu\text{g/mL}$) were served as the positive control. As shown in **Figure 4B**, compound **8a** exhibited fungicidal activity at 2 $\mu\text{g/mL}$. In contrast, FLC didn't show fungicidal activity at high concentration (16 $\mu\text{g/mL}$).

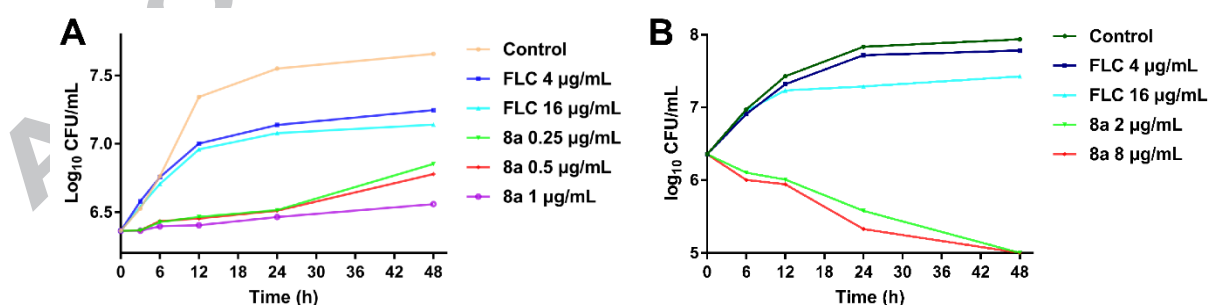


Fig. 4 (A) Time-growth curves of *C. neoformans* H99 obtained by using initial inoculums of 2×10^6 colony-forming units (CFU)/mL. (B) Time-kill curves of *C. neoformans* H99 obtained by using an initial inoculum of 2×10^6 CFU/mL.

3.6. Compound **8a** induced apoptosis of *C. neoformans* H99 cells and arrested cell cycle at the G1/S phase

Apoptosis of *C. neoformans* H99 treated with compound **8a** was investigated by flow cytometry. The percentage of apoptotic cells in the control group was 1.20%. After treating with compound **8a** at 0.5 $\mu\text{g/mL}$, 1 $\mu\text{g/mL}$ and 2 $\mu\text{g/mL}$ for 24 h, the percentage of apoptotic cells was 23.82%, 44.62%, and 57.48%, respectively (**Fig. 5**). The results suggested that compound **8a** could significantly induce apoptosis effect. Then, the effect of the compound **8a** on the cell cycle was investigated using flow cytometric analysis to further clarify the antifungal mechanism. As shown in **Fig. 6**, G1/S arrest was occurred after a 24 h exposure to compound **8a**. In contrast, control group showed 12.24% of cells in G1 phase and 7.89% in S phase. After treated with compound **8a** at 0.5, 1 and 2 $\mu\text{g/mL}$ for 24 h, the ratios in G1 phase were 50.21%, 49.14% and 48.61%, respectively (**Fig. 6**), while the S phase decreased or disappeared. The results indicated that compound **8a** could significantly increase the subpopulation of cells in the G1 phase and reduce the number of cells in the G2 phase resulting in cell cycle arrest at the G1/S phase.

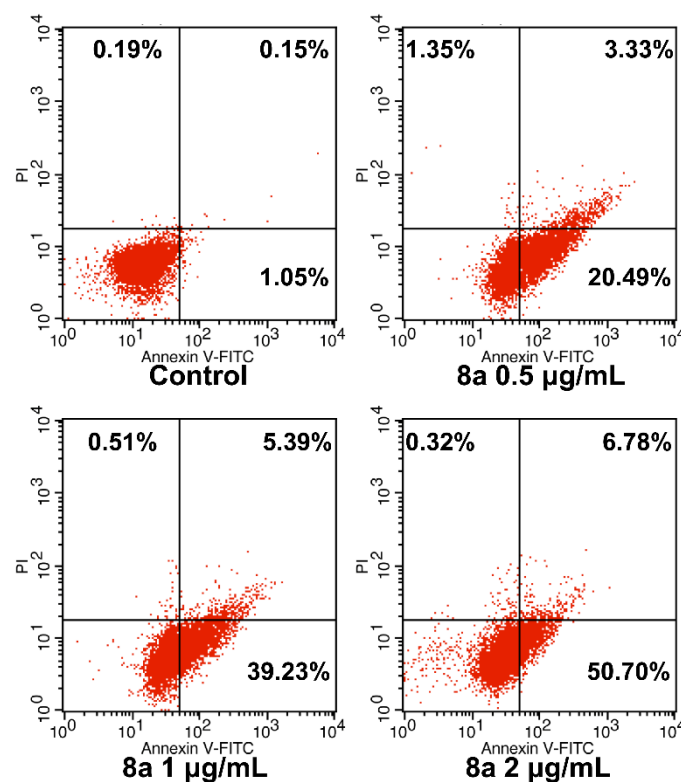


Fig. 5 The effect of compound **8a** on apoptosis in *C. neoformans* H99 cells. *C. neoformans* cells were treated with different concentrations of compound **8a** for 24 h. Flow cytometry was used to examine apoptosis ($n = 3$). Representative photographs of three independent experiments were shown.

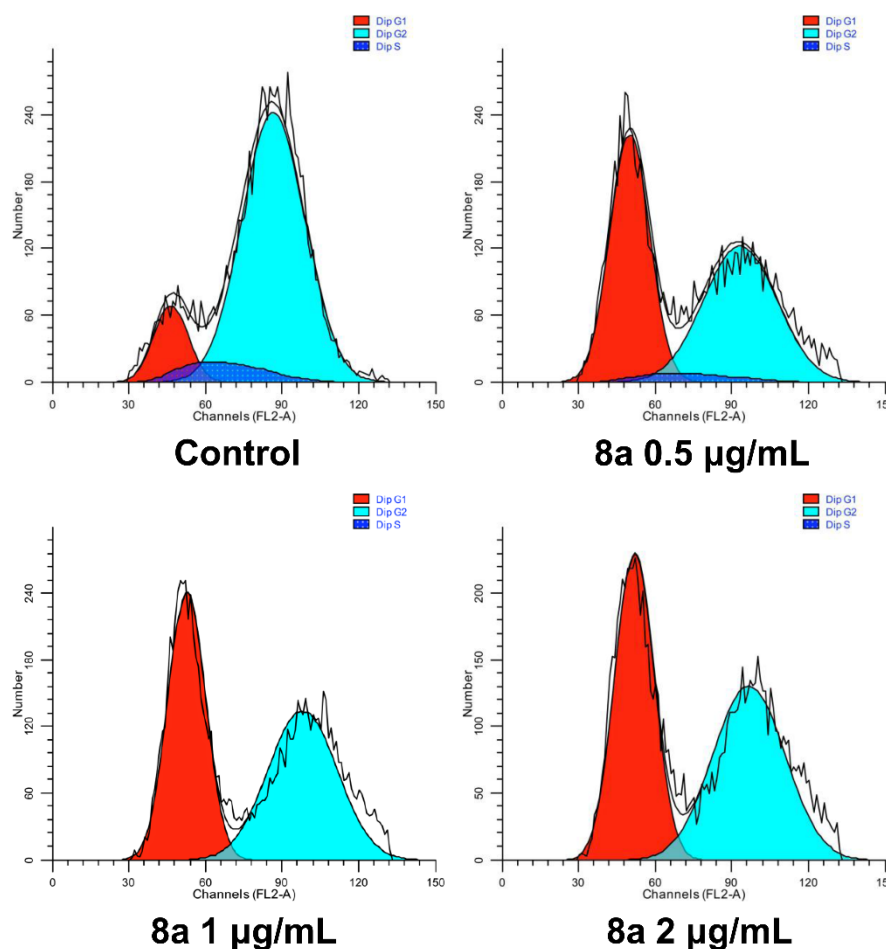


Fig. 6 The effect of compound **8a** on cell cycle in *C. neoformans* H99 cells. Cells treated with different concentrations of compound **8a** for 24 h were assayed by flow cytometry.

4. Conclusions

In summary, starting from antifungal natural product sampangine, a series of simplified tricyclic isoxazole derivatives were designed and synthesized by scaffold hopping. As compared with the lead compounds, the anti-cryptococcal activities of the target compounds were substantially improved. Particularly, compound **8a** showed excellent antifungal activity against *C. neoformans* ($MIC_{80} = 0.031 \mu\text{g/mL}$). Moreover, it was fungicidal and had effective inhibitory effects against important virulence factors (i.e. biofilm, melanin and urease) of *C. neoformans*. It was reported that *o*-vanillin displayed fungicidal activity by triggering oxidative stress, which lead to the disruption of cellular

redox homeostasis and caused mitochondrial dysfunction.²⁵ The melanin could act as a first line of defense against ROS formation.²⁶ It is suggested that inhibition of melanin biosynthesis by fungicide compound **8a** could be related to oxidative stress and mitochondrial dysfunction. In a preliminary investigation of the antifungal mechanism, compound **8a** induced apoptosis and arrest *C. neoformans* cells at the G1/S phase. Similarly, triclosan was reported to induce apoptosis-like death in *C. neoformans* cells.²⁷ Taken together, compound **8a** represents a novel anti-cryptococcal lead compound with a new mode of action. Further lead optimization and target identification studies are ongoing in our lab.

5. Experimental Section

5.1. Chemistry

Bruker AVANCE300 or AVANCE600 spectrometers (Bruker Company, Germany) is used to recorded ¹H NMR and ¹³C NMR spectra, using CDCl₃ or DMSO-*d*₆ as solvents and TMS as an internal standard. The chemical shift are expressed as ppm (δ). Elemental analyses were performed with a MOD-1106 instrument and were consistent with theoretical values within 0.4%. The mass spectral data was recorded on an Esquire 3000 LC-MS mass spectrometer. However, the ion peaks like [M+H]⁺ or [M-H]⁻ cannot be determined for most target compounds. Only HRMS result of compound **8d** were reported herein. Silica gel thin-layer chromatography (TLC) was performed on precoated plates GF-254 (Qingdao Haiyang Chemical, China). The target compound was isolated and purified using a silica gel column (Silica gel 60G, Qingdao Haiyang Chemical, China). Purity of the compounds was analyzed by HPLC (Agilent Technologies 1260 Infinity) using MeOH/H₂O = 70/30 as the mobile phase with a flow rate of 0.5 mL/min. The purity of all compounds was greater than 95%. All solvents and reagents were analytically pure, and no further purification was needed.

All starting materials were commercially available.

5.1.1. 5,5-Dibromo-6,7-dihydrobenzo[*b*]thiophen-4(5*H*)-one (5)

A solution of CuBr₂ (11.3 g, 50.5 mmol) in EtOAc (30 mL) was stirred at 80 °C for 10 min. Then, a solution of 6,7-dihydrobenzo[*b*]thiophen-4(5*H*)-one (1.918 g, 12.6 mmol) in CHCl₃ (10 mL) was added dropwise to the mixture solution (via addition funnel) and stirred for 12 h at 80 °C. Then, the solvent was removed under reduced pressure. The mixture was filtered by celite pad after diluted with EtOAc (40 mL). The filtrate was washed with sat. NaHCO₃ (50 mL × 2), dried over Na₂SO₄, filtrated and concentrated under reduced pressure. The crude product was purified by silica gel chromatography eluted with Hexane/EtOAc = 50/1 to give target compound **6** (3.6 g, yield 92.1%) as a white solid. ¹H NMR (300 MHz, DMSO-*d*₆) δ 7.55 (d, *J* = 5.3 Hz, 1H), 7.38 (d, *J* = 5.3 Hz, 1H), 3.15 (t, *J* = 3.0 Hz, 4H).

5.1.2. 5-Bromobenzo[*b*]thiophen-4-ol (6)

Li₂CO₃ (1.43 g, 19.32 mmol) was added into a solution of 5,5-dibromo-6,7-dihydrobenzo[*b*]thiophen-4(5*H*)-one (1 g, 3.22 mmol) in DMF (30 mL). The mixture was heated at 100 °C and stirred for 3 h under N₂. Then, the reaction mixture was filtered after cooled to room temperature. The filtrates were diluted with H₂O (20 mL) and acidified with 1 N HCl to pH = 1. The resulting solution was extracted with EtOAc (40 mL × 2). The separated organic layer was washed with H₂O (20 mL × 6), dried over Na₂SO₄, filtrated and concentrated under reduced pressure to afford crude product. The residue was purified by column silica gel chromatography (Hexane/EtOAc = 60/1) to give target compound **6** (0.66 g, yield 90.3%) as a white solid. ¹H NMR (300 MHz, DMSO-*d*₆) δ 10.24 (s, 1H), 7.69-7.63 (m, 2H), 7.45 – 7.38 (m, 2H).

5.1.3. 5-Bromobenzo[*b*]thiophene-4,7-dione (7)

To a solution of 5-bromobenzo[*b*]thiophen-4-ol (0.5 g, 2.18 mmol) in AcOH (4 mL) and TFA (5 mL) and a few drops of water, PhI(OAc)₂ (2.11 g, 6.55 mmol) was added in portions during a period of 30 min at 0 °C. Then, the mixture was stirred at 0 °C for 10 min and then at room temperature for 20 min. Then, MeOH (12.5 mL) was added into the solution and stirred for 10 min. The mixture was diluted with H₂O (20 mL) and extracted by DCM (40 mL×2). The combined organic layer was washed with sat. NaCl (20 mL × 2), dried over Na₂SO₄, filtrated and concentrated under reduced pressure to afford crude product. The residue was purified by silica gel column chromatography (Hexane/EtOAc = 60/1) to give target compound **7** (0.37 g, yield 69.7%) as a yellow solid. ¹H NMR (600 MHz, CDCl₃) δ 7.70 (d, *J* = 5.1 Hz, 1H), 7.63 (d, *J* = 5.0 Hz, 1H), 7.39 (s, 1H).

5.1.4. 3-Methylthieno[3',2':4,5]benzo[1,2-*d*]isoxazole-4,8-dione (**8a**)

To a solution of 5-bromobenzo[*b*]thiophene-4,7-dione (0.125 g, 0.51 mmol) in DCM (10 mL) was added dropwise Et₃N (18 uL) and an aqueous solution of NaClO (15 mL, 7.5%) at 0 °C. Then, a solution of propionaldehyde oxime (53 mg, 0.72 mmol) in DCM (5 mL) was added dropwise into the mixture during a period of 15 min. After the TLC showed the starting material was consumed completely, the mixture was diluted with H₂O (20 mL) and extracted by DCM (40 mL × 2). The combined organic phase was washed with sat. NaCl (20 mL × 2). Then, the organic layer was separated, dried over Na₂SO₄, filtered and concentrated under reduced pressure. The residue was purified by silica gel column chromatography (Hexane/EtOAc = 60/1) to give target compound **8a** (70 mg, yield 61.6%) as a yellow solid. ¹H NMR (300 MHz, CDCl₃) δ 7.75 (d, *J* = 5.1 Hz, 1H), 7.67 (d, *J* = 5.1 Hz, 1H), 3.06 (q, *J* = 7.5 Hz, 2H), 1.41 (t, *J* = 7.5 Hz, 3H). ¹³C NMR (151 MHz, CDCl₃) δ 174.17, 168.96, 166.12, 163.14, 145.89, 140.77, 134.35, 126.46, 120.38, 19.24, 11.84. HPLC purity: 99.3%.

The synthetic methods for compounds **8b-t** were similar to the synthesis of compound **8a**.

5.1.5. 3-Propylthieno[3',2':4,5]benzo[1,2-d]isoxazole-4,8-dione (8b)

Yellow solid (0.123 g, yield 60.9%). ¹H NMR (300 MHz, CDCl₃) δ 7.75 (d, *J* = 5.1 Hz, 1H), 7.67 (d, *J* = 5.1 Hz, 1H), 3.01 (t, *J* = 7.4 Hz, 2H), 1.92-1.78 (m, 2H), 1.04 (t, *J* = 7.4 Hz, 3H). ¹³C NMR (151 MHz, CDCl₃) δ 174.19, 168.95, 166.09, 161.95, 145.92, 140.75, 134.35, 126.46, 120.48, 27.20, 20.86, 13.72. HPLC purity: 95.8%.

5.1.6. 3-(Methoxymethyl)thieno[3',2':4,5]benzo[1,2-d]isoxazole-4,8-dione (8c)

Yellow solid (22 mg, yield 42.7%). ¹H NMR (600 MHz, CDCl₃) δ 7.77 (d, *J* = 5.1 Hz, 1H), 7.68 (d, *J* = 5.0 Hz, 1H), 4.86 (s, 2H), 3.54 (s, 3H). ¹³C NMR (151 MHz, CDCl₃) δ 173.43, 168.59, 166.22, 158.36, 145.61, 140.76, 134.65, 126.52, 120.34, 64.37, 59.33.

5.1.7. 3-(Pyridin-4-yl)thieno[3',2':4,5]benzo[1,2-d]isoxazole-4,8-dione (8d)

Yellow solid (84 mg, yield 36.6%). ¹H NMR (300 MHz, CDCl₃) δ 8.83 (d, *J* = 6.0 Hz, 2H), 8.12 (d, *J* = 6.1 Hz, 2H), 7.81 (d, *J* = 5.1 Hz, 1H), 7.71 (d, *J* = 5.1 Hz, 1H). ¹³C NMR (151 MHz, CDCl₃) δ 173.17, 168.39, 167.66, 158.80, 150.34, 146.54, 140.18, 135.18, 133.97, 126.41, 123.12, 119.66. HRMS (ESI, negative) *m/z*: [M + H]⁺ calcd for C₁₄H₆N₂O₃S, 283.0172; found 283.0176, HPLC purity: 99.4%.

5.1.8. 3-(Pyridin-2-yl)thieno[3',2':4,5]benzo[1,2-d]isoxazole-4,8-dione (8e)

Yellow solid (56 mg, yield 48.8%). ¹H NMR (300 MHz, CDCl₃) δ 8.87 (d, *J* = 4.8 Hz, 1H), 8.23 (d, *J* = 7.8 Hz, 1H), 7.96 (t, *J* = 7.7 Hz, 1H), 7.78 (d, *J* = 5.1 Hz, 1H), 7.70 (d, *J* = 5.1 Hz, 1H), 7.57 – 7.50 (m, 1H). ¹³C NMR (75 MHz, CDCl₃) δ 172.95, 168.63, 167.24, 159.90, 150.10, 146.73, 145.77, 140.16, 137.25, 134.80, 126.32, 125.65, 125.30, 119.79.

5.1.9. 3-(*o*-Tolyl)thieno[3',2':4,5]benzo[1,2-d]isoxazole-4,8-dione (8f)

Yellow solid (0.168 g, yield 77.0%). ^1H NMR (300 MHz, CDCl_3) δ 7.76 (d, $J = 5.1$ Hz, 1H), 7.70 (d, $J = 5.1$ Hz, 1H), 7.48 – 7.43 (m, 2H), 7.38 – 7.30 (m, 2H), 2.35 (s, 3H). ^{13}C NMR (151 MHz, CDCl_3) δ 173.23, 168.93, 166.37, 160.52, 146.35, 140.49, 137.66, 134.50, 130.68, 130.65, 130.32, 126.36, 125.77, 125.36, 120.58, 20.17.

5.1.10. 3-(2-Bromophenyl)thieno[3',2':4,5]benzo[1,2-d]isoxazole-4,8-dione (8g)

Yellow solid (0.217 g, yield 73.5%). ^1H NMR (600 MHz, CDCl_3) δ 7.77–7.76 (m, 2H), 7.71 (d, $J = 5.1$ Hz, 1H), 7.51 – 7.42 (m, 3H). ^{13}C NMR (151 MHz, CDCl_3) δ 172.69, 168.83, 166.10, 159.95, 146.05, 140.59, 134.60, 133.22, 132.06, 131.39, 127.64, 127.46, 126.44, 123.47, 120.92.

5.1.11. 3-(2-Fluorophenyl)thieno[3',2':4,5]benzo[1,2-d]isoxazole-4,8-dione (8h)

Yellow solid (64 mg, yield 52.1%). ^1H NMR (600 MHz, CDCl_3) δ 7.76 (d, $J = 5.1$ Hz, 1H), 7.70 (d, $J = 5.1$ Hz, 1H), 7.69 – 7.66 (m, 1H), 7.60 – 7.56 (m, 1H), 7.33 – 7.27 (m, 2H). ^{13}C NMR (151 MHz, CDCl_3) δ 172.70, 168.74, 166.45, 160.54 (d, $J_{\text{C-F}} = 253.3$ Hz), 156.02, 146.34, 140.43, 134.53, 133.08 (d, $J_{\text{C-F}} = 8.4$ Hz), 131.13, 126.37, 124.34 (d, $J_{\text{C-F}} = 3.3$ Hz), 120.60, 116.24 (d, $J_{\text{C-F}} = 20.9$ Hz), 114.50 (d, $J_{\text{C-F}} = 14.2$ Hz).

5.1.12. 3-(2-Chlorophenyl)thieno[3',2':4,5]benzo[1,2-d]isoxazole-4,8-dione (8i)

Yellow solid (0.1 g, yield 78.0%). ^1H NMR (300 MHz, CDCl_3) δ 7.77 (d, $J = 5.1$ Hz, 1H), 7.71 (d, $J = 5.1$ Hz, 1H), 7.61 – 7.50 (m, 3H), 7.45 – 7.41 (m, 1H). ^{13}C NMR (151 MHz, CDCl_3) δ 172.70, 168.81, 166.16, 158.65, 146.11, 140.55, 134.56, 134.22, 132.01, 131.31, 130.05, 126.90, 126.42, 125.59, 121.02.

5.1.13. 3-(2-Methoxyphenyl)thieno[3',2':4,5]benzo[1,2-d]isoxazole-4,8-dione (8j)

Yellow solid (84 mg, yield 65.7%). ^1H NMR (600 MHz, CDCl_3) δ 7.71 (d, J = 5.0 Hz, 1H), 7.67 (d, J = 5.1 Hz, 1H), 7.55 – 7.51 (m, 1H), 7.49 (dd, J = 7.5, 1.6 Hz, 1H), 7.09 – 7.04 (m, 2H), 3.81 (s, 3H).

5.1.14. 3-(*m*-Tolyl)thieno[3',2':4,5]benzo[1,2-*d*]isoxazole-4,8-dione (**8k**)

Yellow solid (99 mg, yield 81.9%). ^1H NMR (300 MHz, CDCl_3) δ 7.97 – 7.91 (m, 2H), 7.76 (d, J = 5.1 Hz, 1H), 7.69 (d, J = 5.1 Hz, 1H), 7.46 – 7.36 (m, 2H), 2.47 (s, 3H). ^{13}C NMR (75 MHz, CDCl_3) δ 173.50, 168.85, 167.24, 160.84, 146.95, 140.07, 138.51, 134.56, 132.15, 129.76, 128.60, 126.53, 126.24, 125.88, 119.47, 21.44.

5.1.15. 3-(3-Methoxyphenyl)thieno[3',2':4,5]benzo[1,2-*d*]isoxazole-4,8-dione (**8l**)

Yellow solid (87 mg, yield 68.0%). ^1H NMR (300 MHz, CDCl_3) δ 7.79 – 7.75 (m, 3H), 7.70 (d, J = 5.1 Hz, 1H), 7.45 (t, J = 8.2 Hz, 1H), 7.15 – 7.09 (m, 1H), 3.92 (s, 3H). ^{13}C NMR (75 MHz, CDCl_3) δ 173.47, 168.81, 167.34, 160.62, 159.69, 147.00, 140.00, 134.63, 129.79, 127.16, 126.23, 121.63, 119.47, 117.84, 114.17, 55.51.

5.1.16. 3-(3-Bromophenyl)thieno[3',2':4,5]benzo[1,2-*d*]isoxazole-4,8-dione (**8m**)

Yellow solid (0.213 g, yield 72.3%). ^1H NMR (300 MHz, CDCl_3) δ 8.37 (s, 1H), 8.14 (d, J = 7.8 Hz, 1H), 7.80 (d, J = 5.1 Hz, 1H), 7.72 – 7.70 (m, 2H), 7.43 (t, J = 8.0 Hz, 1H). ^{13}C NMR (75 MHz, CDCl_3) δ 173.37, 168.64, 167.41, 159.48, 146.73, 140.11, 134.92, 134.38, 132.14, 130.25, 127.95, 126.33, 122.74, 119.37.

5.1.17. 3-(3-Chlorophenyl)thieno[3',2':4,5]benzo[1,2-*d*]isoxazole-4,8-dione (**8n**)

Yellow solid (0.1 g, yield 78.2%). ^1H NMR (300 MHz, CDCl_3) δ 8.22 (s, 1H), 8.09 (d, J = 7.6 Hz, 1H), 7.80 (d, J = 5.1 Hz, 1H), 7.71 (d, J = 5.1 Hz, 1H), 7.58 – 7.45 (m, 2H). ^{13}C NMR (75 MHz,

CDCl_3) δ 173.37, 168.64, 167.42, 159.60, 146.74, 140.11, 134.90, 134.79, 131.47, 130.02, 129.32, 127.74, 127.49, 126.33, 119.38.

5.1.18. 3-(4-Methoxyphenyl)thieno[3',2':4,5]benzo[1,2-d]isoxazole-4,8-dione (**8o**)

Yellow solid (88 mg, yield 69.5%). ^1H NMR (300 MHz, CDCl_3) δ 8.15 (d, J = 8.9 Hz, 2H), 7.76 (d, J = 5.1 Hz, 1H), 7.69 (d, J = 5.0 Hz, 1H), 7.04 (d, J = 8.8 Hz, 2H), 3.90 (s, 3H). ^{13}C NMR (75 MHz, CDCl_3) δ 173.71, 168.89, 167.25, 162.07, 160.32, 147.02, 140.04, 134.49, 130.98, 126.22, 119.34, 118.37, 114.13, 55.43.

5.1.19. 3-(*p*-Tolyl)thieno[3',2':4,5]benzo[1,2-d]isoxazole-4,8-dione (**8p**)

Yellow solid (0.199 g, yield 82.4%). ^1H NMR (300 MHz, CDCl_3) δ 8.04 (d, J = 8.1 Hz, 2H), 7.76 (d, J = 5.1 Hz, 1H), 7.69 (d, J = 5.1 Hz, 1H), 7.34 (d, J = 8.0 Hz, 2H), 2.45 (s, 3H). ^{13}C NMR (75 MHz, CDCl_3) δ 173.58, 168.89, 167.23, 160.70, 146.97, 141.81, 140.06, 134.54, 129.43, 129.23, 126.24, 123.14, 119.45, 21.60.

5.1.20. 3-(4-Bromophenyl)thieno[3',2':4,5]benzo[1,2-d]isoxazole-4,8-dione (**8q**)

Yellow solid (0.206 g, yield 70.0%). ^1H NMR (300 MHz, CDCl_3) δ 8.08 (d, J = 8.5 Hz, 2H), 7.79 (d, J = 5.1 Hz, 1H), 7.72 - 7.67 (m, 3H). ^{13}C NMR (75 MHz, CDCl_3) δ 173.48, 168.66, 167.41, 159.85, 146.75, 140.11, 134.86, 132.04, 130.84, 126.33, 126.17, 124.99, 119.36.

5.1.21. 3-(1-Methyl-1H-pyrrol-2-yl)thieno[3',2':4,5]benzo[1,2-d]isoxazole-4,8-dione (**8r**)

Yellow solid (8 mg, yield 22.8%). ^1H NMR (600 MHz, CDCl_3) δ 7.75 (d, J = 5.1 Hz, 1H), 7.69 (d, J = 5.1 Hz, 1H), 7.65 - 7.64 (m, 1H), 6.90 - 6.88 (m, 1H), 6.32 - 6.31 (m, 1H), 4.00 (s, 3H). ^{13}C NMR (151 MHz, CDCl_3) δ 173.17, 168.91, 166.32, 153.47, 147.41, 139.76, 134.21, 128.93, 126.04, 119.14, 118.78, 118.55, 108.73, 37.88.

5.1.22. 3-(Thiophen-2-yl)thieno[3',2':4,5]benzo[1,2-d]isoxazole-4,8-dione (**8s**)

Yellow solid (56 mg, yield 47.8%). ^1H NMR (300 MHz, CDCl_3) δ 8.53 (d, $J = 3.7$ Hz, 1H), 7.78 (d, $J = 5.1$ Hz, 1H), 7.70 (d, $J = 5.1$ Hz, 1H), 7.57 (d, $J = 5.1$ Hz, 1H), 7.23 (dd, $J = 5.0, 3.9$ Hz, 1H). ^{13}C NMR (75 MHz, CDCl_3) δ 173.36, 168.60, 167.14, 155.42, 146.71, 140.03, 134.70, 133.49, 130.21, 128.03, 127.03, 126.32, 118.82.

5.1.23. 3-(Thiophen-3-yl)thieno[3',2':4,5]benzo[1,2-d]isoxazole-4,8-dione (**8t**)

Yellow solid (23 mg, yield 39.1%). ^1H NMR (300 MHz, CDCl_3) δ 8.87 (d, $J = 2.8$ Hz, 1H), 7.87 (d, $J = 5.0$ Hz, 1H), 7.78 (d, $J = 5.1$ Hz, 1H), 7.70 (d, $J = 5.1$ Hz, 1H), 7.46 (dd, $J = 5.1, 3.0$ Hz, 1H). ^{13}C NMR (151 MHz, $\text{DMSO}-d_6$) δ 174.35, 169.29, 168.07, 155.65, 146.61, 140.73, 136.88, 131.17, 128.38, 127.16, 126.94, 126.35, 119.00.

5.2 Biology

5.2.1. In Vitro Antifungal Activity Assay

In vitro antifungal activity was measured by the serial dilution method in 96-well microtest plates. *C. albicans* strains SC5314, *C. neoformans* strains H99, *C. Gattii* strains ATCC14116 and *C. neo. var. Grubii* strains ATCC34877 was used in this study. MIC was measured according to the requirements of National Committee for Clinical Laboratory Standards (NCCLS). RPMI 1640 (Gibco BRL) buffered with 0.165M MOPS (Sigma), NaHCO_3 (0.2%) and NaOH (0.27%) was used as the test medium. All strains were routinely grown in YPD with 1% yeast extract (BD), 2% peptone (BD) and 2% D-Glucose (Sangon Biotech) liquid medium at 30 °C in a shaking incubator. Briefly, the initial concentration of fungal suspension in RPMI 1640 medium was 10^3 CFU/mL, and tested compounds were dissolved in DMSO. The yeast strains were incubated at 35 °C for 48 h.

5.2.2. In Vitro Biofilm Formation Assay

The experimental procedure was performed according to the reported method with a few

modification.²⁸ The suspension of *C. neoformans* H99 cells (1.0×10^6 CFU/mL in RPMI 1640 medium) was added into a 96-well tissue culture plate (Corning, USA) and allowed to incubate at 37 °C for 90 minutes. After that, the upper culture medium and the non-adherent cells were removed. Fresh RPMI 1640 medium with or without drugs was added into after the adherent cells had been washed three times with PBS. A drug-free sample was served as a control. Concentrations for compounds **8a** and **8b** and AMB were 0.062-8 µg/mL. Then the plates were incubated for a further 24 h at 37 °C. The biofilm formation rate was calculated by using an XTT reduction assay.

5.2.3. Melanin and Urease Production Assay

Exponentially growing *C. neoformans* H99 cells were harvested, washed three times with PBS, and resuspended in RPMI 1640 medium at 1×10^6 cells/mL. Different concentrations of compound **8a** and FLC were added into the suspension. Cell suspension containing different concentrations of drugs was dropped onto the L-DOPA or urea medium and incubated at 37 °C to detect the production of melanin and urease.

5.2.4. Time-growth Curve Assay

Time-growth curve assay was performed according to the reported method with a few modifications.²⁹ Briefly, exponentially growing *C. neoformans* H99 cells were harvested and resuspended in fresh RPMI 1640 medium 5 mL to a concentration of 2×10^6 cells/mL. Various concentrations of compound **8a** were added. The sample were cultured at 30 °C under constant shaking (200 rpm). A portion of the cell suspension was removed and counted at the indicated time points (0h, 3 h, 6 h, 9 h, 12 h, 24 h, 48 h). DMSO was added into the control group. Three independent experiments were performed.

5.2.5. Fungicidal Activity Assay

Time-kill curves were used to evaluate the fungicidal activity of compound **8a**. The experimental operation was carried out according to the reported method.²⁸ Exponentially growing *C. neoformans* H99 cells were washed with PBS (1 mL \times 3), then resuspended with RPMI 1640 medium to 2×10^6 cells/mL in 5 mL. Different concentrations of the compound **8a** and FLC were added and the sample was cultured at 30 °C under constant shaking (200 rpm). A portion of the cell suspension was removed at the indicated time points (0h, 6h, 12 h, 24 h, 48 h) and diluted to appropriate folds. The diluent cell suspension was plated on SDA agar medium to determine the concentration after incubation for 48 h at 30 °C.

5.2.6. Cell Cycle Analysis by Flow Cytometry

The experimental procedure was performed according to the reported method with a few modification.³⁰ Exponentially growing *C. neoformans* H99 cells were harvested, washed three times with PBS, and resuspended in RPMI 1640 medium (20 mL) at 5×10^5 cells/mL. Different concentrations of compound **8a** were added into the suspension. After cultured at 30 °C under constant shaking (200 rpm) for 24 h, each sample was centrifuged, washed with PBS three times. Each 10 mg cells (wet weight) were resuspended with 100 mL PBS (containing 0.24% snailase) and then incubated for 1 h at 30 °C to break the cell wall. The sample was washed with PBS twice and fixed with 70% ethanol overnight. The cells were then stained with 50 μ g/mL of propidium iodide (PI) at 4 °C for 30 min. About 1×10^6 cells were measured using a FACSCalibur cytometer (Becton, Dickinson, San Jose, CA).

5.2.7. Cell Apoptosis Detection by Flow Cytometry

The preparation procedure of the sample treated with different concentrations of compound **8a** was similar as the step of cell cycle assay. After the sample had been resuspended in binding buffer

400 μ L, it was then added to 5 μ L of annexin V-FITC and incubated at room temperature for 15 min. Then, 10 μ L of PI was added into the suspensions and incubated for another 15 min at room temperature. The cells were analyzed by a flow cytometer (Becton, Dickinson, San Jose, CA).

Acknowledgments

This work was supported by the National Natural Science Foundation of China (Grants 81725020 to C. S.), Science and Technology Commission of Shanghai Municipality (Grant 17XD1404700) and National Natural Science Foundation of China (Grants 21502224 to N. L.).

A. Supplementary data

Supplementary data associated with this article can be found, in the online version, at XXXX.

References

1. Brown GD, Denning DW, Levitz SM. *Science*. 2012;336:647.
2. Denning DW, Bromley MJ. *Science*. 2015;347:1414-1416.
3. Spitzer M, Robbins N, Wright GD. *Virulence*. 2017;8:169-185.
4. Sloan DJ, Parris V. *Clin Epidemiol*. 2014;6:169-182.
5. Liu TB, Perlin DS, Xue C. *Virulence*. 2012;3:173-181.
6. Park BJ, Wannemuehler KA, Marston BJ, et al. *AIDS*. 2009;23:525-530.
7. Rajasingham R, Smith RM, Park BJ, et al. *Lancet Infect Dis*. 2017;17:873-881.
8. Williamson PR, Jarvis JN, Panackal AA, et al. *Nat Rev Neurol*. 2017;13:13-24.
9. Nixon GL, McEntee L, Johnson A, et al. *Antimicrob Agents Chemother*. 2018;62.
10. Shaw KJ, Schell WA, Covell J, et al. *Antimicrob Agents Chemother*. 2018;62.
11. Ogundeji AO, Porotloane BF, Pohl CH, et al. *Antimicrob Agents Chemother*. 2018;62.
12. Coelho C, Casadevall A. *Cell Microbiol*. 2016;18:792-799.
13. Perfect JR. *Nat Rev Drug Discov*. 2017;16:603-616.
14. Liu N, Wang C, Su H, et al. *Future Med Chem*. 2016;8:1435-1454.
15. Liu N, Tu J, Dong G, et al. *J Med Chem*. 2018;61:5484-5511.
16. Di Santo R. *Nat Prod Rep*. 2010;27:1084-1098.
17. Xiao Z, Morris-Natschke SL, Lee KH. *Med Res Rev*. 2016;36:32-91.
18. Jiang Z, Liu N, Dong G, et al. *Bioorg Med Chem Lett*. 2014;24:4090-4094.
19. Jiang Z, Liu N, Hu D, et al. *Chem Commun*. 2015;51:14648-14651.
20. Liu N, Zhong H, Tu J, et al. *Eur J Med Chem*. 2018;143:1510-1523.

21. Li DD, Zhao LX, Mylonakis E, et al. *Antimicrob Agents Chemother.* 2014;58:2344-2355.
22. Cenci E, Bistoni F, Mencacci A, et al. *Cell Microbiol.* 2004;6:953-961.
23. Brilhante RSN, Espana JDA, de Alencar LP, et al. *Mycoses.* 2017;60:697-702.
24. Pini G, Faggi E, Campisi E. *Rev Iberoam Micol.* 2017;34:77-82.
25. Kim JH, Lee HO, Cho YJ, et al. *PloS one.* 2014;9:e89122.
26. Kothamasi D, Wannijn J, Van Hees M, et al. *J Environ Radioactiv.* 2019;197:16-22.
27. Movahed E, Tan GM, Munusamy K, et al. *Front Microbiol.* 2016;7:360.
28. Wang S, Wang Y, Liu W, et al. *ACS Med Chem Lett.* 2014;5:506-511.
29. Huang Y, Dong G, Li H, et al. *J Med Chem.* 2018;61:6056-6074.
30. Li DD, Xu Y, Zhang DZ, et al. *Antimicrob Agents Chemother.* 2013;57:6016-6027.

Graphical Abstract

Discovery of Novel Simplified Isoxazole Derivatives of Sampangine as potent Anti-cryptococcal Agents

Zhuang Li^{1,†}, Na Liu^{2,†}, Jie Tu², Changjin Ji², Guiyan Han², Yan Wang^{2,*}, Chunquan Sheng^{1,2,*}

